Data in Brief 41 (2022) 107841

Contents lists available at ScienceDirect

Data in Brief

journal homepage: www.elsevier.com/locate/dib

Data Article

Fabrication data of two light-responsive systems to release an antileishmanial drug activated by infrared photothermal heating

Letícia S. Vitorino[a], Thiago C. dos Santos[a], Isabela A.A. Bessa[a], Evelyn C.S. Santos[a,d], Brunno R.F. Verçoza[b], Luiz Augusto S. de Oliveira[c], Juliany C.F. Rodrigues[b], Célia M. Ronconi[a,*]

[a] *Departamento de Química Inorgânica, Universidade Federal Fluminense, Campus do Valonguinho, Niterói-RJ, 24020-150, Brazil*
[b] *Núcleo Multidisciplinar de Pesquisa em Biologia (NUMPEX-Bio), Campus UFRJ-Duque de Caxias Prof. Geraldo Cidade, Universidade Federal do Rio de Janeiro, Duque de Caxias, RJ, Brazil*
[c] *Núcleo Multidisciplinar de Pesquisa em Nanotecnologia (NUMPEX-Nano), Campus UFRJ-Duque de Caxias Prof. Geraldo Cidade, Universidade Federal do Rio de Janeiro, Duque de Caxias, RJ, Brazil*
[d] *Present address: Centro Brasileiro de Pesquisas Físicas, Urca-RJ, 22290-180, Brazil*

ARTICLE INFO

Article history:
Received 5 January 2022
Revised 10 January 2022
Accepted 14 January 2022
Available online 19 January 2022

Keywords:
Drug delivery systems enhanced by NIR light
reduced graphene oxide based materials
pluronic P123
P123
polyethylenimine
leishmaniasis

ABSTRACT

The data provided in this study are related to the fabrication of two light-responsive systems based on reduced graphene oxide (rGO) functionalized with the polymers Pluronic P123 (P123), rGO-P123, and polyethyleneimine (PEI), rGO-PEI, and loaded with amphotericin B (AmB), an antileishmanial drug. Here are described the experimental design to obtain the systems and characterization methods, such as Attenuated Total Reflectance-Fourier Transform Infrared Spectroscopy (ATR-FTIR), Raman Spectroscopy, Powder X-Ray Diffraction, Transmission Electron Microscopy, Scanning Electron Microscopy and Thermogravimetric Analyses. Also, AmB spectroscopy studies are described. The materials rGO-P123 and rGO-PEI were loaded with AmB and the optimization of AmB and polymer fragments structures revealed several possible hydrogen bonds formed between the materials and the drug. The drug release was analyzed with

DOI of original article: 10.1016/j.colsurfb.2021.112169
* Corresponding author.
E-mail address: cmronconi@id.uff.br (C.M. Ronconi).
Social media: @RonconiCelia (C.M. Ronconi)

https://doi.org/10.1016/j.dib.2022.107841

and without Near-Infrared (NIR) light. In the studies conducted under NIR light irradiation for 10 min, an infrared lamp was disposed at 64 cm from the samples and an optical fiber thermometer was employed to measure the temperature variation. Cytotoxicity studies and antiproliferative assays against *Leishmania amazonensis* promastigotes were evaluated. The complete work data entitled Amphotericin-B-Loaded Polymer-Functionalized Reduced Graphene Oxides for *Leishmania amazonensis* Chemo-Photothermal Therapy have been published to Colloids and Surfaces B: Bionterfaces (https://doi.org/10.1016/j.colsurfb.2021.112169) [1].

Specifications Table

Subject	*Materials Science*
Specific subject area	*Biomaterials*
Type of data	Tables Figures Equations Graphs
How the data were acquired	Thermo Scientific Nicolet iS50 FTIR spectrometer Bruker D8 ADVANCE X-ray diffractometer Shimadzu TGA-60 Witec Alpha 300 system JEOL JEM-1011 microscope JEOL JSM 7100F microscope Cary 60 UV-Vis Spectrophotometer (Varian). LEICA DMI 6000 Smartphone digital camera ChemDraw Professional 16.0 Origin versions 7.0 and 8.0
Data format	Raw Analysed
Description of data collection	ATR-FTIR spectra were collected in a range of 500–4000 cm^{-1}, resolution of 4 cm^{-1} and 64 scans. Cu Kα radiation at room temperature was used to collect PXRD data. TGA analyses were obtained in the range temperature of 30 to 600 °C under N_2 atmosphere. Raman data were acquired with an excitation green laser (λ = 532 nm) equipped with a lens glass of 50x. TEM data were obtained in a microscope with an acceleration voltage of 80 kV. SEM images were obtained using a field emission gun SEM microscope with working voltage of 15 kV. UV-Vis spectra were acquired in a quartz cuvette and PBS and DMSO as solvent.
Data source location	*Universidade Federal Fluminense, Niterói, RJ, Brazil* *Universidade Federal do Rio de Janeiro, Duque de Caxias, RJ, Brazil*
Data accessibility	Raw data was deposited at Mendeley Data database under accession doi:10.17632/nbrjytd6bh.1 https://data.mendeley.com/datasets/nbrjytd6bh/1
Related research article	L.S. Vitorino, T.C. dos Santos, I.A.A. Bessa, E.C.S. Santos, B.R.F. Verçoza, L.A.S. de Oliveira, J.C.F. Rodrigues, C.M. Ronconi, Amphotericin-B-Loaded Polymer-Functionalized Reduced Graphene Oxides for Leishmania amazonensis Chemo-Photothermal Therapy. Colloid Surface B 209 (2022) 112169-112178, doi:10.1016/j.colsurfb.2021.112169.

Value of the Data

- The data present details on the synthetic procedure and chemical characterization of two materials based on reduced graphene oxide functionalized with two polymers, Pluronic P123 and polyethyleneimine.
- Leishmaniasis, as tropical neglected disease, does not receive enough attention from public health systems worldwide. Therefore, these data may encourage the scientific community to invest in leishmaniasis treatment.
- Reduced graphene oxide can absorb light in near infrared region and converts it into heat. This photothermal property can improve the drug release and parasite death.
- The AmB release is improved by a cheap NIR light source, providing a new possible treatment for cutaneous leishmaniasis.

1. Data Description

1.1. Preparation and characterization of rGO-P123 and rGO-PEI

To prepare rGO-P123 and rGO-PEI we used graphene oxide (GO) obtained from a procedure previously described by our group based on modified Hummer's method [1,2]. GO was further reduced with hydrazine in the presence of poly(ethylene glycol)-*block*-poly(propylene glycol)-*block*-poly(ethylene glycol) (PEO_{20}–PPO_{70}–PEO_{20}, Pluronic® P123) or branched polyethyleneimine (PEI). GO reduction to rGO can regenerate the sp^2 carbon network improving the π-conjugated system and increasing the NIR light absorption [3]. Therefore, on one hand rGO is a better photothermic agent than GO but on the other hand, rGO has lower colloidal stability in aqueous media because its surface is more hydrophobic than GO surface. To improve rGO colloidal stability in aqueous media, Pluronic® P123 or PEI were used to coat the rGO surfaces. Pluronic® P123 (Fig. 1(a)) is a biocompatible amphiphilic triblock copolymer formed by a central hydrophobic chain of propylene oxide (70 units) and two hydrophilic chains on its sides composed of polyethylene oxide (20 units each) [4]. This polymer is approved by the Food and Drug

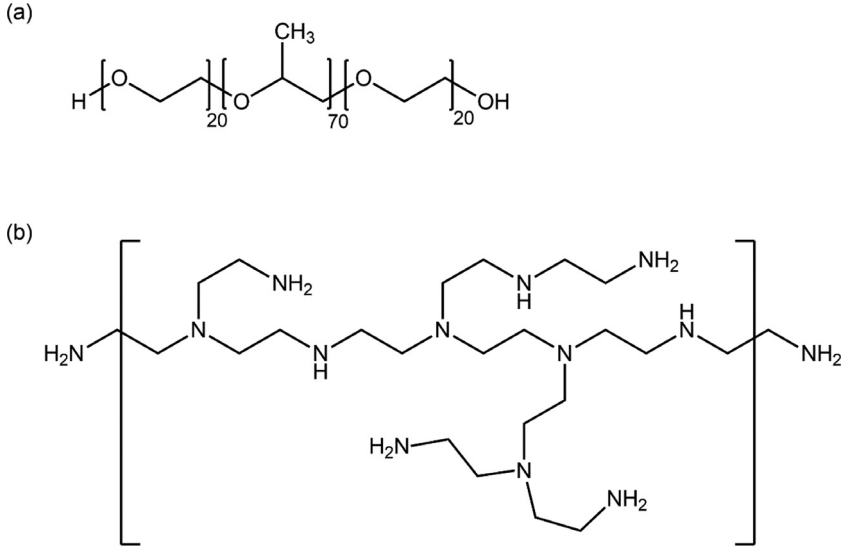

Fig. 1. Structural representation of (a) Pluronic® P123 and (b) PEI.

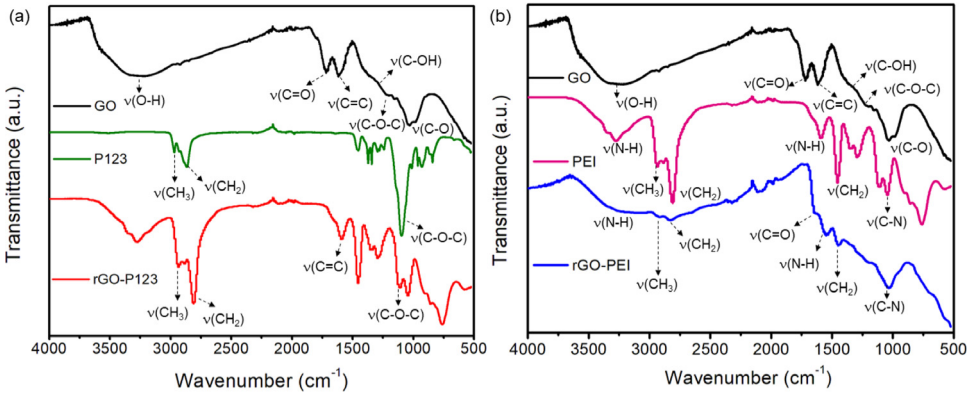

Fig. 2. ATR-FTIR spectra of (a) rGO-P123 and (b) rGO-PEI and their precursors.

Administration (FDA) and has been used in pharmaceutical formulations including transport of low molecular weight drugs and polypeptides, due to its ability to increase the solubility of hydrophobic drugs [5]. Pluronic® P123 can interact with rGO by its central hydrophobic chain of propylene oxide moiety [6]. Branched PEI (Fig. 1(b)) is a biocompatible water-soluble polymer containing primary, secondary and tertiary amines and can behave as a reducing agent and surface modifier [7]. In acid medium, the amino groups can be protonated and the polymer becomes cationic [8]. Because of the positive surface charge of different materials functionalized with PEI, cell uptake efficiency can be improved [9]. This polymer has been widely applied in regenerative medicine and gene therapy as deliver expression systems [10]. PEI can interact with rGO by covalent bonds and/or electrostatic interactions [7].

ATR-FTIR spectra of GO, P123, PEI, rGO-P123 and rGO-PEI are shown in Figs. 2 (a) and (b). GO spectrum shows absorption bands at 3268, 1719, 1618, and 1201 cm^{-1} attributed to stretching vibrations of hydroxyl (O-H), carbonyl (C=O), alkene (C=C) and epoxide groups (C-O-C), respectively [19]. The bands at 1378 and 1037 cm^{-1} are O-H deformation of the group C-OH and C-O stretching vibration, respectively [7]. The spectrum of rGO-P123 shows characteristic absorptions of the Pluronic® P123 at 2970, 2860 and 1080 cm^{-1} assigned to $\nu(CH_3)$, $\nu(CH_2)$ and ν(C-O-C), respectively [11]. The spectrum of rGO-PEI shows bands at 3150, 2910, 2810 and 1030 cm^{-1} ascribed to the stretching vibrations of ν(N-H), $\nu(CH_3)$, $\nu(CH_2)$ and ν(C-N), respectively [12]. In addition, the bands at 1540 and 1456 cm^{-1} are due to the N–H bend vibration and CH_2 from the PEI. Therefore, the ATR-FTIR results confirm the presence of the P123 and PEI on rGO surface. A comparison between GO and rGO-P123 spectra displays a significant decrease in band intensities of carbonyl and epoxy groups in the latter spectrum, suggesting these groups were partially reduced by hydrazine in rGO-P123. In the rGO-PEI spectrum, the band associated with epoxy groups almost disappears compared to GO suggesting its reduction by hydrazine was more effective in the presence of PEI; most likely because PEI also acts as a reducing agent. Liu *et al.* proposed some possible mechanisms for the reduction of epoxy, hydroxyl, carbonyl and carboxylic groups of GO by PEI [7]. The proposed mechanism for the reduction of epoxy groups by PEI is similar to the one proposed by hydrazine. For the carbonyl groups, they suggested Michael addition/Schiff base reaction with the amino groups of PEI. For the hydroxyl groups, they proposed that *trans*-hydroxyl could form epoxy groups followed by reduction, whereas *cis*-hydroxyl and terminal hydroxyl groups do not react. In the rGO-PEI spectrum, one can see a band at 1645 cm^{-1} indicating amide formation due to the carboxylic reduction in GO by PEI, suggesting the polymer is covalently bonded on rGO surface [13]. Furthermore, the disappearance of O-H stretching vibration in rGO-PEI spectrum, which was observed at 1378 cm^{-1} in GO spectrum, suggests that hydroxyl groups were reduced by PEI. The presence of AmB on the rGO-P123-AmB

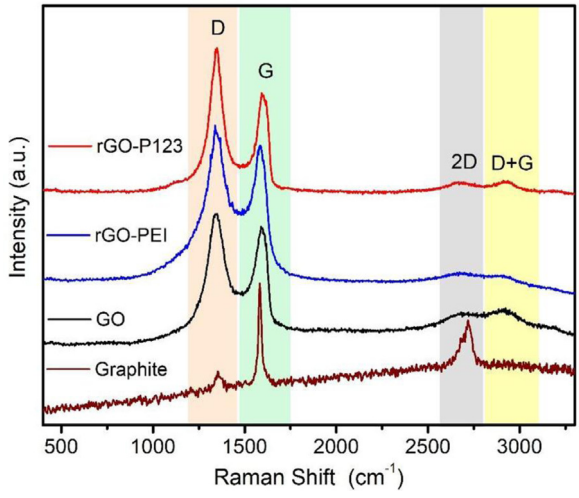

Fig. 3. Raman spectra of rGO-P123 and rGO-PEI and their precursors.

Table 1
Wavenumbers of D and G Raman bands observed in the spectra showed in Fig. 3, as well as their intensity ratios.

Material	D band (cm^{-1})	G band (cm^{-1})	I_D/I_G
Graphite	1350	1581	0.14
GO	1344	1597	1.14
rGO-P123	1347	1594	1.49
rGO-PEI	1339	1584	1.15

and rGO-PEI-AmB materials was confirmed by ATR-FTIR spectra (Fig. 14). The main bands of AmB in the ATR-FTIR spectra are showed in Table 2. The

Raman spectra of graphite, GO, rGO-P123 and rGO-PEI are shown in Fig. 3. In the graphite spectrum, the band at 1350 cm^{-1} (D band) associated to A_{1g} breathing mode is related to defects, such as vacancies, grain boundaries and amorphous carbon species; the band at 1581 cm^{-1} (G band) is due to the in-plane E_{2g} stretching vibrations of the sp^2 carbon; whereas the band at 2727 cm^{-1} (2D band) is associated to graphite bulk structure [7]. The D band of GO shifts to 1343 cm^{-1} and its intensity (I_D) significantly increases due to the oxidation process, which introduced oxygen-functional groups on the carbon layers, such as hydroxyl, carbonyl and epoxy groups, as shown in the ATR-FTIR spectrum of GO, Figs. 2(a) and (b). The G band in rGO-P123 (1594 cm^{-1}) and rGO-PEI (1584 cm^{-1}) shifts to lower wavenumbers compared to GO (1597 cm^{-1}), indicating the reduction of this material [14].

The wavenumbers of D and G bands as well as the intensity ratio between these bands (I_D/I_G) for all materials are displayed in Table 1. The intensity ratios (I_D/I_G) are 1.14 (GO), 1.49 (rGO-P123) and 1.15 (rGO-PEI). I_D/I_G ratio is indicative of the disorder level in graphene derivatives, which can be associated with defects, impurities and an average size of the sp^2 domains in these materials. The I_D/I_G ratio can also be used to confirm the presence of carbon atom with sp^3 hybridization originated from the grafted polymers on the graphene platforms [7].

The higher ratio (I_D/I_G) of GO (1.14) than graphite (0.14) confirms the oxidation of carbon sheets decreasing the sp^2 domain. ATR-FTIR spectra (Figs. 2(a) and (b)) showed removal of oxygen functionalities therefore a decrease in the ratio (I_D/I_G) of rGO-P123 and rGO-PEI in comparison with GO is expected. However, rGO-P123 (1.49) and rGO-PEI (1.15) showed higher ratios (I_D/I_G) than GO (1.14), which might be due to the presence of the polymers on the carbon sheets. The band at 2925 cm^{-1} (D+G combination mode) in the GO, rGO-PEI and rGO-P123 spectra is

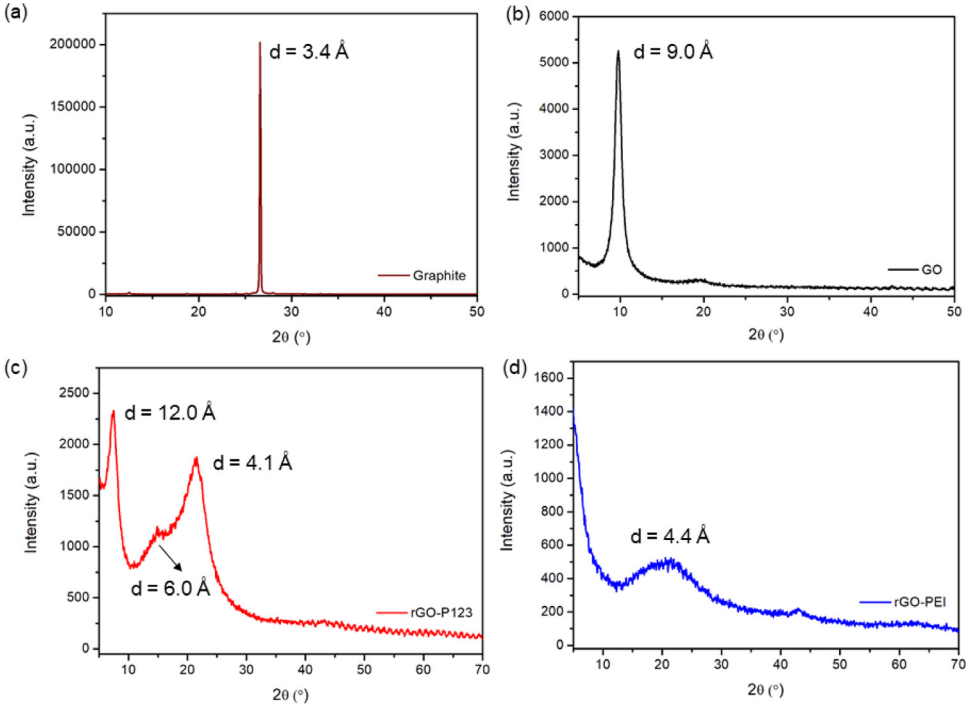

Fig. 4. PXRD patterns of (a) graphite, (b) GO, (c) rGO-P123 and (d) rGO-PEI.

associated with system disorder [15]. The increase of I_D/I_G ratios is related to the decrease of Csp^2 and the increase of defects (Csp^3) present within the carbon network.

Powder X-ray diffraction (PXRD) of graphite shows a narrow peak at $2\theta = 26.6$ ° corresponding to an interlayer distance (d-spacing) of 3.4 Å, Fig. 4(a). In PXRD of GO, this peak widens and shifts to $2\theta = 9.8$ ° (Fig. 4 (b)) indicating a d-spacing of 9.0 Å due to the introduction of oxygen-containing functional groups (see ATR-FTIR spectrum of GO, Figs. 2(a) and (b)). rGO-PEI shows a broad peak at $2\theta = 20.2$ ° ($d = 4.4$ Å) due to chemical reduction, which decreased the amount of oxygen-containing functional groups and reestablished the conjugated π-network of GO (Fig. 4(d)) [7]. The powder pattern diffraction of rGO-P123 exhibits a broad diffraction peak at $2\theta = 7.4$ ° (d = 12.0 Å) (Fig. 4(c)). This peak suggests the presence of residual GO. In addition, two other peaks at 14.7 ° ($d = 6.0$ Å) and 21.4 ° ($d = 4.1$ Å) could indicate that oxygen-functional groups were removed from GO surface with different degree of efficiency.

TEM images (Figs. 5 and 6) showed a two-dimensional morphology composed of thin, wrinkled and overlapping sheet-like structures of rGO-P123 and rGO-PEI. The wrinkled sheets is indicative that the materials were reduced [16].

SEM images (Figs. 7 and 8) of rGO-P123 and rGO-PEI revealed smooth, folded and crumpled sheet-like structures [17].

TGA curves of rGO-P123, rGO-PEI and their precursors are displayed in Figs. 9(a) and (b). GO shows three decomposition steps: i) under 100 °C due to adsorbed water molecules on GO surface; ii) from 124 to 228 °C as a result of the decomposition of oxygen-containing functional groups and iii) above 300 °C due to the carbonic chain decomposition [7]. The rGO-P123 and rGO-PEI materials showed different thermal decomposition behavior compared with GO. The rGO-P123 curve (Fig. 9(a)) revealed two weight loss steps: i) the first one, at the temperature range of 173 to 388 °C, can be associated with decomposition of the polymer (Pluronic® P123) and ii) the second one, in the temperature range of 355 to 502 °C, can be related to the pyrolysis

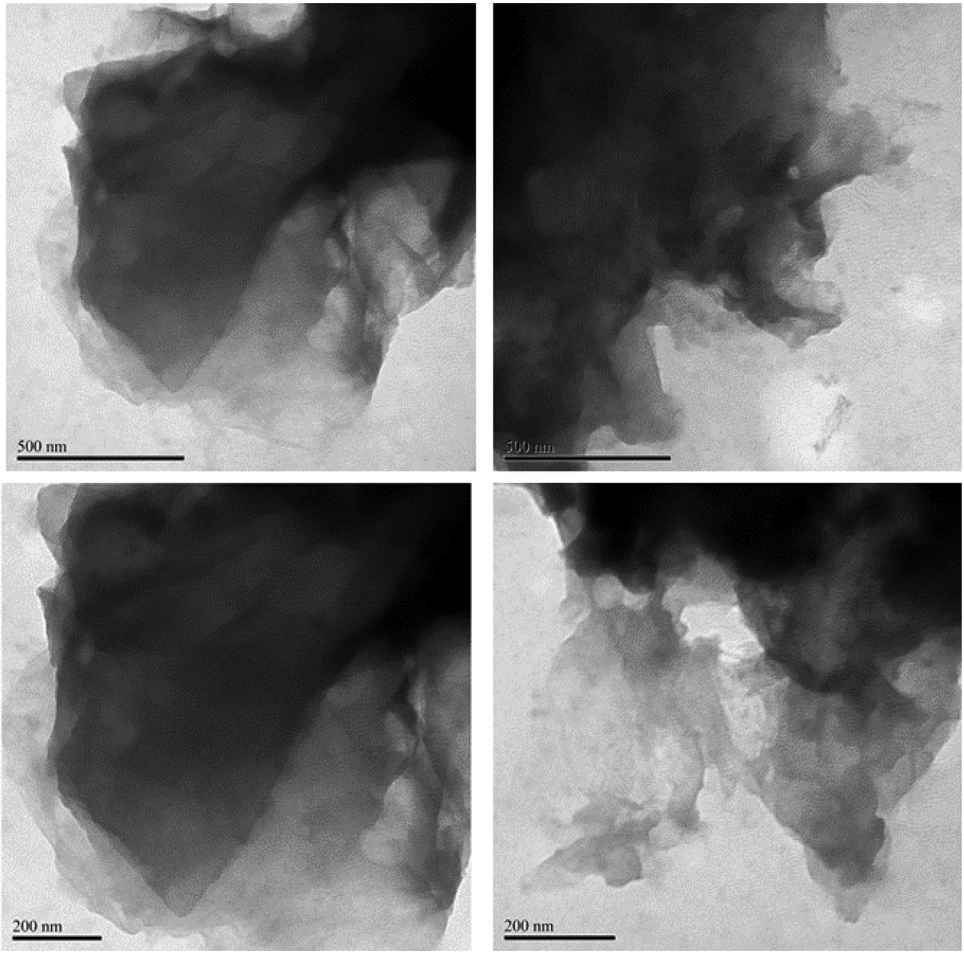

Fig. 5. TEM images of rGO-P123.

of the rGO carbonic chain. The rGO-PEI TGA curve (Fig. 9(b)) exhibited a weight loss at 100 °C related to adsorbed water molecules on the material surface. For rGO-PEI, the weight loss in the range of 100 to 350 °C is associated with decomposition of physiosorbed and covalently bonded PEI molecules, as shown the amide linkage ascribed by the band at 1645 cm^{-1} in ATR-FTIR spectrum of rGO-PEI (Fig. 2(b)) [7]. In the range of 365 to 587 °C of rGO-PEI TGA curve occurs the decomposition of the rGO carbon skeleton. The quantity of polymers incorporated in each material was estimated by TGA analyses. An amount of 2.43 mg mg^{-1} of Pluronic® P123 was anchored on the surface of rGO to obtain rGO-P123, while 0.78 mg mg^{-1} of PEI recovered the rGO surface to yield rGO-PEI.

During the reduction process using hydrazine monohydrated and the functionalization with the polymers, the GO dispersion color changed from bright brown to black, which indicates that the materials were successfully reduced (Fig. 10).

AmB is an anthracycline antibiotic that shows activity against fungi and parasitic diseases such as leishmaniasis. This drug presents an amphiphilic structure formed by a side composed by hydroxyl groups and another moiety containing seven unsaturated bonds forming a hydrophobic portion (Fig. 11).

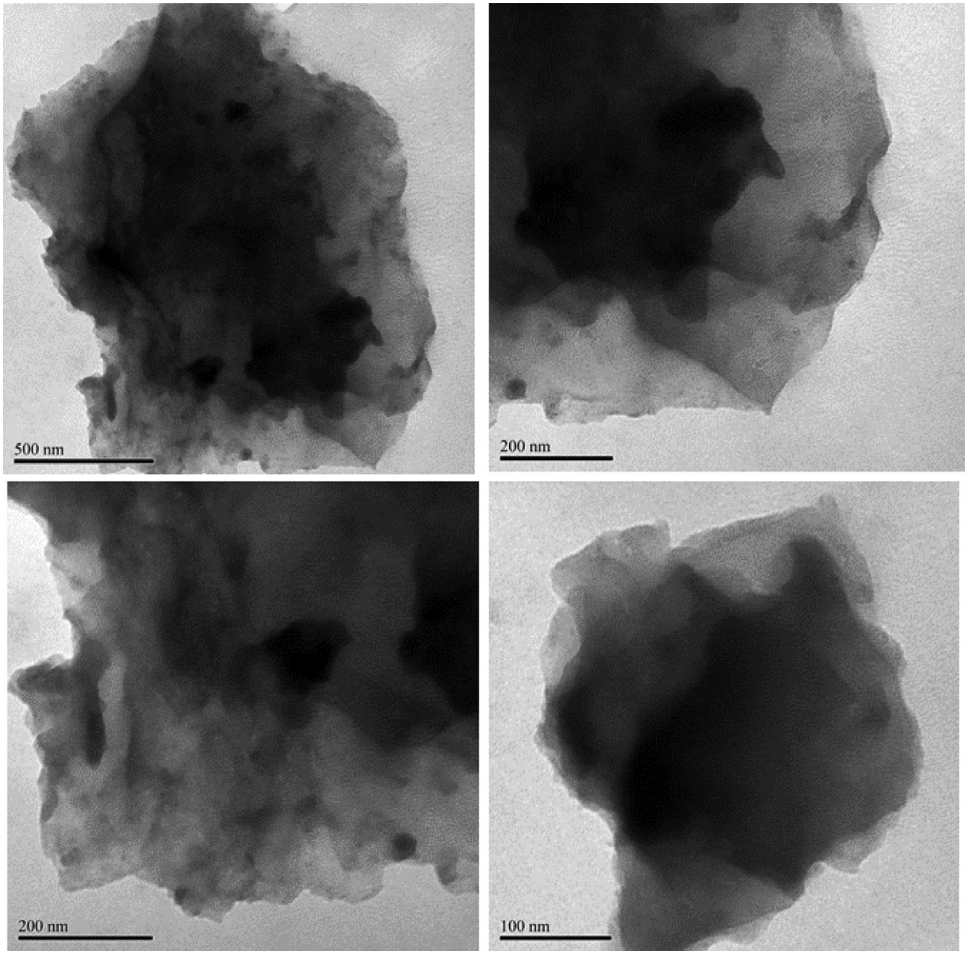

Fig. 6. TEM images of rGO-PEI.

To ensure AmB will be in its monomeric form, several solvent mixtures of PBS and DMSO were studied (Fig. 12).

The possible hydrogen bonds formed between AmB and the polymer fragments were investigated by optimizing their structures using MM2 method from ChemDraw Professional 16.0 software.

The optimization shows one bifurcated hydrogen bond formed between AmB and rGO-P123, as shown in Fig. 13(a). This interaction is formed between the hydroxyl group from AmB and two ether groups from P123 molecule, forming a five membered ring (interaction I). Concerning rGO-PEI and AmB, the optimization shows one hydrogen bond between the secondary amino group of PEI and the hydroxyl group from AmB molecule (O-H···N, interaction I'); one hydrogen bond between the primary amino group of PEI and the hydroxyl group from AmB molecule (HN-H···O, interaction II'); two bifurcated hydrogen bonds between one secondary amino group from PEI and AmB hydroxyl group resulting in a $R_2^2(4)$ supramolecular synthon (interaction III'). The interaction IV' involves two primary amino groups one from AmB and another from PEI (Fig. 13(b)). The macrophage interaction with rGO-PEI, rGO-P123, rGO-PEI-AmB and rGO-P123-AmB materials are represented in Fig. 15.

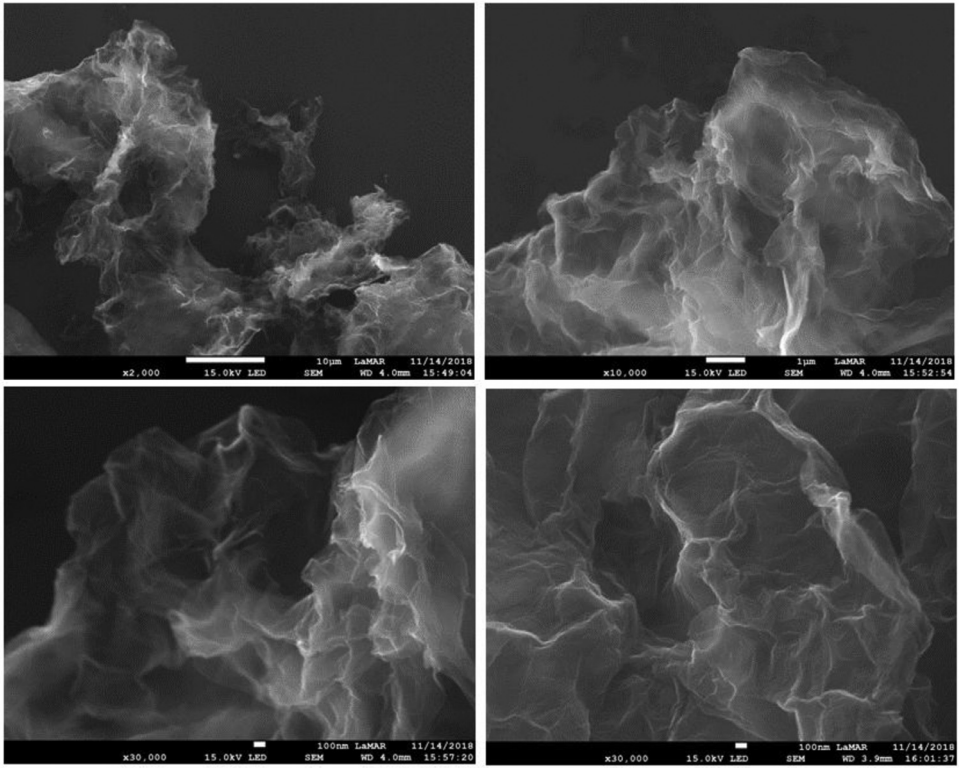

Fig. 7. SEM images of rGO-P123.

Table 2
Wavenumbers of absorption bands observed in the spectra showed in Fig. 14(a) and (b).

Wavenumber (cm^{-1}) AmB	rGO-P123-AmB	rGO-PEI-AmB	Band Assignments
3363	3316	3304	ν(O-H)
1691	1722	1728	ν(C=O)
1006	1085	1010	ν(C-O)

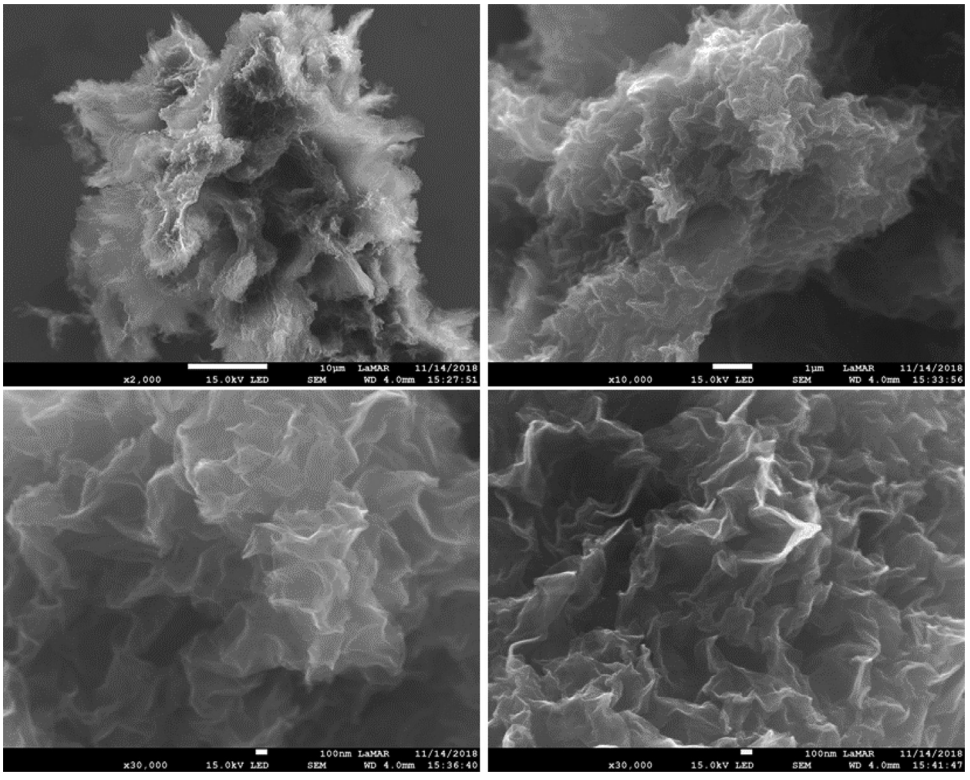

Fig. 8. SEM images of rGO-PEI.

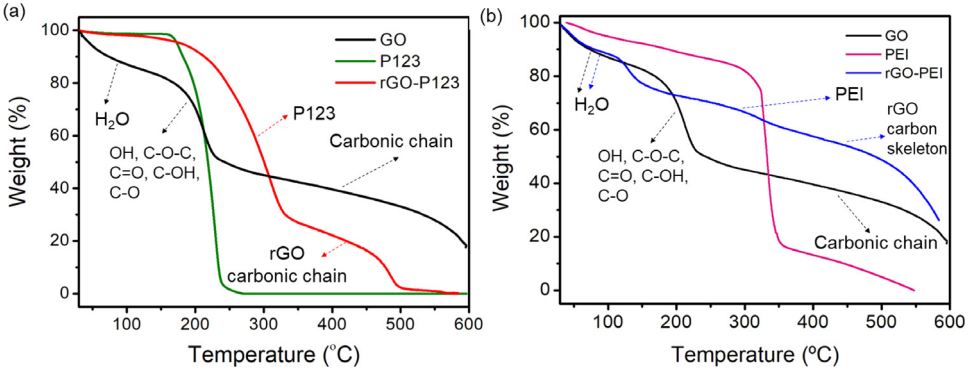

Fig. 9. TGA curves of (a) rGO-P123 and (b) rGO-PEI and their precursors.

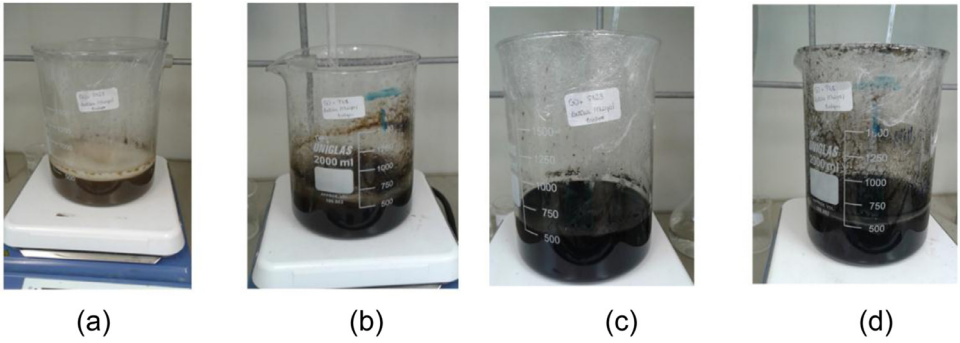

Fig. 10. GO aqueous dispersions after addition of (a) Pluronic® P123 and (b) PEI. Dispersions after the addition of hydrazine, resulting in (c) rGO-P123 and (d) rGO-PEI.

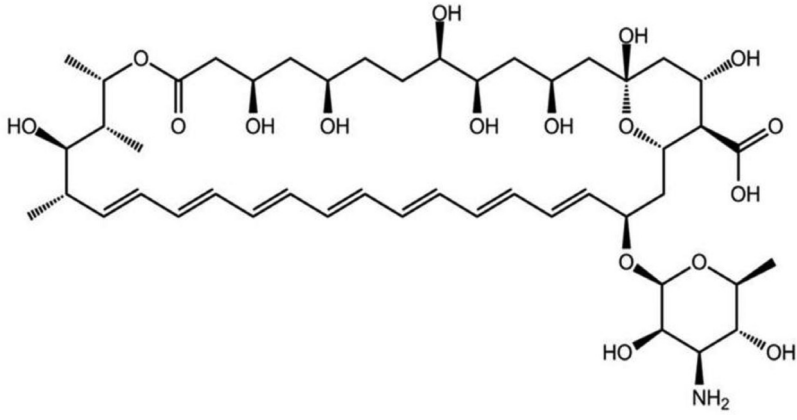

Fig. 11. Structural representation of AmB.

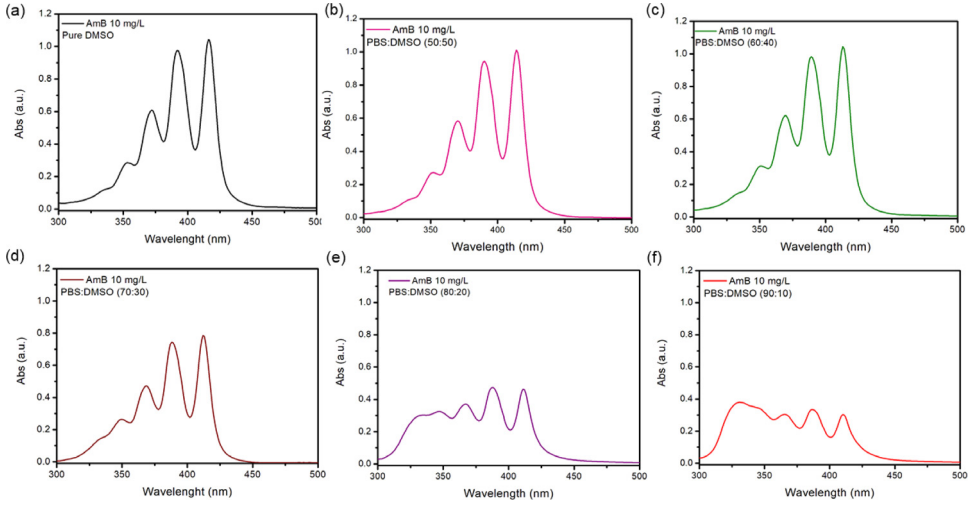

Fig. 12. UV-vis spectra of AmB dispersed in different proportions of PBS:DMSO: (a) pure DMSO, (b) PBS:DMSO (50:50), (c) PBS:DMSO (60:40), (d) PBS:DMSO (70:30), (e) PBS:DMSO (80:20) and (f) PBS:DMSO (90:10).

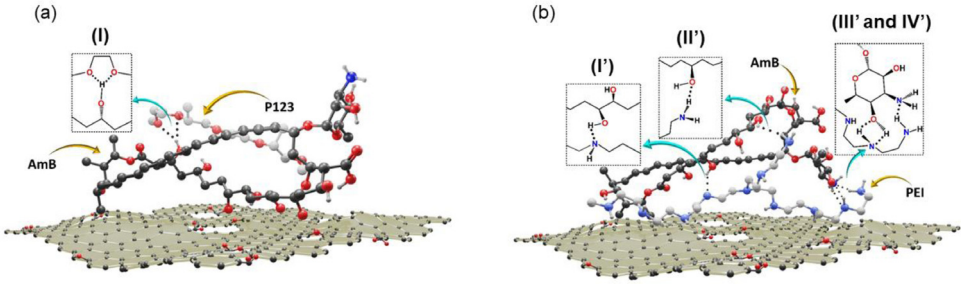

Fig. 13. Representation of possible hydrogen bonds formed between AmB and (a) rGO-P123 and (b) rGO-PEI.

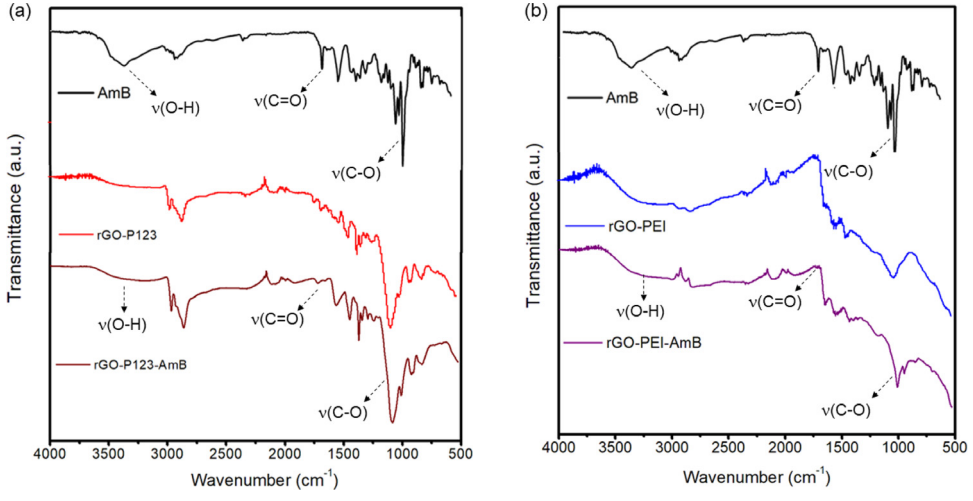

Fig. 14. ATR-FTIR spectra of (a) rGO-P123-AmB and (b) rGO-PEI-AmB.

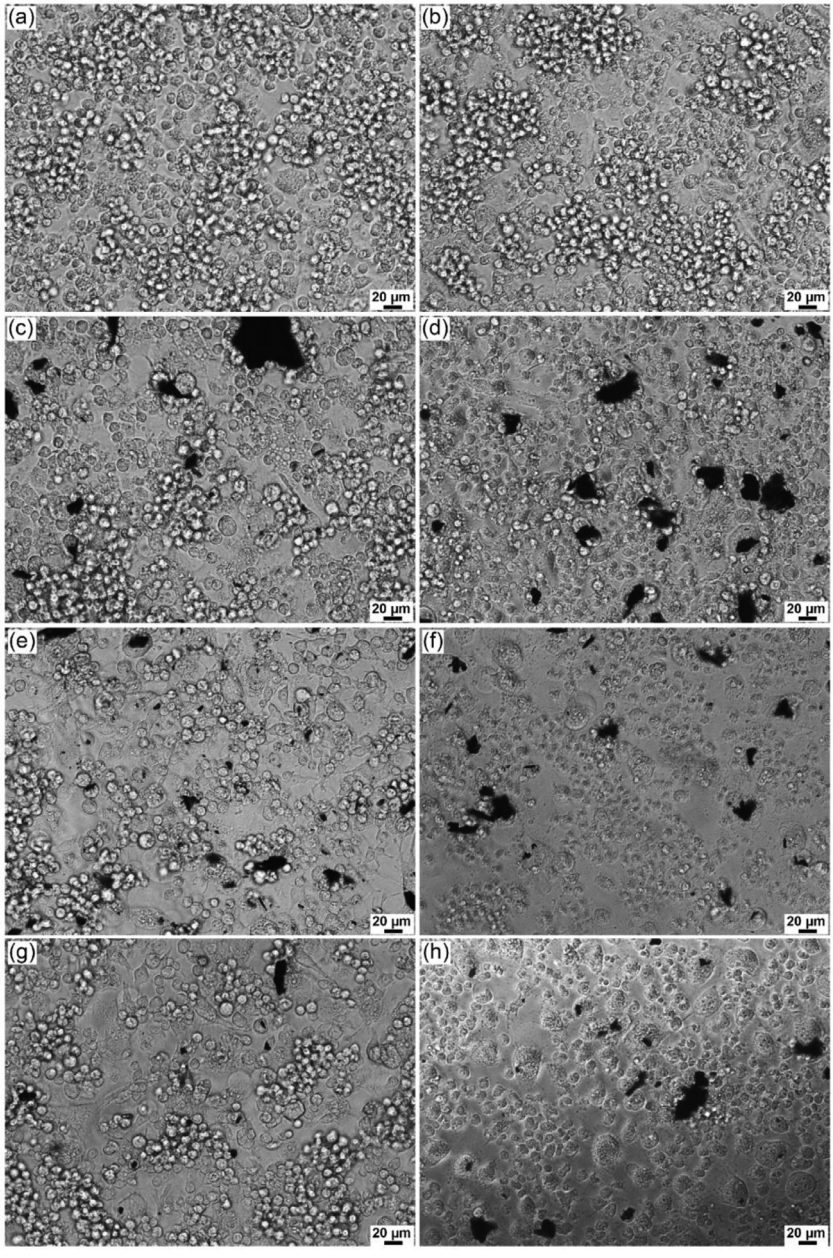

Fig. 15. Phase-contrast optical microscopy images of RAW264.7 macrophages: (a) control and (b) PBS:DMSO (60:40) control and after 72 h of treatment with (c) rGO-PEI 5 μg mL^{-1}, (d) rGO-P123 5 μg mL^{-1}, (e) rGO-PEI 15 μg mL^{-1}, (f) rGO-P123 15 μg mL^{-1}, (g) rGO-PEI-AmB 5 μg mL^{-1} and (h) rGO-P123-AmB 5 μg mL^{-1} .

2. Experimental Design, Materials and Methods

2.1. Preparation of graphene oxide water dispersion

Graphite was first pre-oxidized following a procedure described in the literature with minor modifications [18]. Briefly, $K_2S_2O_8$ (2.5 g, 9.25 mmol) and P_2O_5 (2.5 g, 17.6 mmol) were completely dissolved in concentrated H_2SO_4 (7.5 mL, 140.7 mmol) at 80 °C under stirring. Then, graphite (5.0 g, 416.3 mmol) was added to the resulting solution and the mixture was under stirring for 3 h. After this period, the solid was dispersed in 1 L of distilled water under stirring for 90 min. The dispersion was filtered, washed with distilled water (up to pH = 7) and dried at room temperature to originate the pre-oxidized graphite as a bright dark-gray solid (6.2 g). The second oxidation step was carried out following a modified Hummer's method [2]. H_2SO_4 (115 mL, 2.16 mol) was transferred to a 3 L beaker in an ice/water bath, then the pre-oxidized graphite (6.18 g) and $NaNO_3$ (2.57 g, 30.2 mmol) were added under stirring. Small portions of $KMnO_4$ (15.1 g, 95.4 mmol) were slowly added, and at the end, the ice/water bath was removed, and the dispersion remained stirring for 3 h at 35 °C. Distilled water (230 mL) was added and the dispersion was heated at 98 °C for further 15 min. The dispersion was cooled to room temperature, and H_2O_2 (20 mL) was slowly added and the mixture remained stirring overnight. The resulting dispersion was filtered, washed with 10% (v/v) HCl (3 x) and dried at room temperature to yield 10.3 g of graphite oxide as a bright brown solid. A dispersion containing 4 mg mL^{-1} of graphite oxide in distilled water was exfoliated in a sonication bath for 2 h and then centrifuged at 5000 rpm for 40 min. The solid was collected and the exfoliation and centrifugation processes were repeated several times up to obtain a dispersion of graphene oxide (GO) without any precipitated solid.

2.2. Preparation of reduced graphene oxide functionalized with P123 (rGO-P123) and PEI (rGO-PEI)

The preparations of rGO-P123 and rGO-PEI were carried out following a procedure from the literature with modifications [19]. Briefly, 200 mL of GO dispersion (4 mg mL^{-1}) was sonicated for 70 min and then equally divided in two portions. To each portion under stirring, 200 mL of distilled water was added, followed by dropwise addition of 100 mL of Pluronic® P123 (11 mg mL^{-1}) aqueous solution in one flask, and 100 mL of PEI solution (19 mg mL^{-1}) in the second flask. Both dispersions were under stirring for further 3 h at room temperature. After this period, 6 mL of hydrazine monohydrate was dropwise added to each flask and then heated at 45 °C for 24 h with continuous stirring to reduce the materials. The solids were collected by filtration, washed with distilled water (up to pH = 7-8) to remove the excess of hydrazine and polymers. The purification of the dispersions was carried out by dialysis (72 h) using 2 L of distilled water and changing it 3 times. The purified dispersions were lyophilized (24 h) to yield black solids named rGO-P123 (539.3 mg) and rGO-PEI (273.34 mg).

2.3. AmB loading on rGO-P123 and rGO-PEI

The samples rGO-P123 and rGO-PEI loaded with amphotericin B (AmB) resulted in the materials named rGO-P123-AmB and rGO-PEI-AmB. AmB-loaded materials were prepared by adding 200 mg of rGO-P123 to 200 mL of AmB solution (100 mg L^{-1}) and 150 mg of rGO-PEI to 150 mL of AmB solution (100 mg L^{-1}) composed of a mixture of phosphate-buffered solution (PBS) and DMSO (60:40). The dispersions were sonicated for 90 min protected from light and then stirred at RT for 24 h. After this period, the dispersions were centrifuged at 5000 rpm for 5 min and the excess of AmB was removed by successive centrifugation and washing steps (Fig. 16). The solids were collected and lyophilized (24 h) yielding the products rGO-P123-AmB (212.8 mg) and rGO-PEI-AmB (165.0 mg).

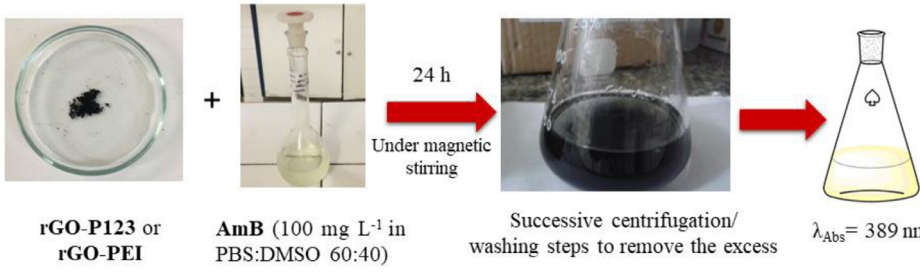

$$\text{AmB-loading efficiency (LE)}\ \% = \left(\frac{m}{M_0}\right) \text{x } 100 \text{ (eqn 1)}$$

Fig. 16. Representation of the AmB-loading process on the materials.

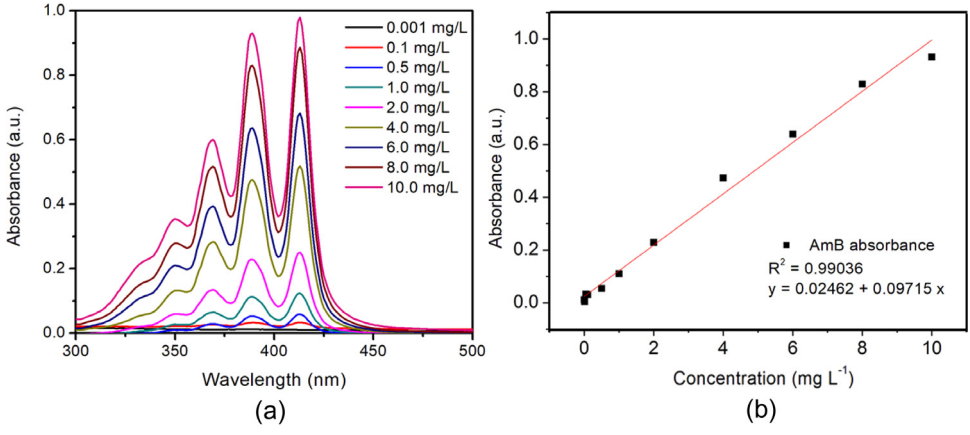

Fig. 17. (a) Absorption spectra of AmB at different concentrations in PBS:DMSO (60:40) obtained at RT and (b) the standard curve of AmB obtained from the absorption spectra using the absorption maximum at λ = 389 nm. This standard curve was used to estimate the amount of AmB loaded and released from rGO-P123-AmB and rGO-PEI-AmB.

Table 3
AmB-loading efficiencies on the materials.

Material	AmB initial mass, M_0 (mg)	AmB-loaded mass, m (mg)	LE%	Loading (mg mg^{-1})
rGO-P123-AmB	20.0	16.32	81.6	0.078
rGO-PEI-AmB	15.0	12.96	86.4	0.086

The supernatants and washing water without rGO were collected and analyzed by UV-Vis spectroscopy to calculated the amounts of AmB loaded on both materials through a standard curve prepared by measuring a series of concentrations of AmB solutions in PBS:DMSO (60:40) at λ = 389 nm (Fig. 17).

The AmB-loading efficiencies were calculated using eqn (1), where M_0 is the initial mass of AmB in the solution (20 mg for rGO-P123 and 15 mg for rGO-PEI) and m is the loaded AmB mass per 100 mg of rGO-P123 or rGO-PEI (Fig. 16). AmB loading efficiency (%) = (m/M_0) × 100 (eqn 1) (Table 3).

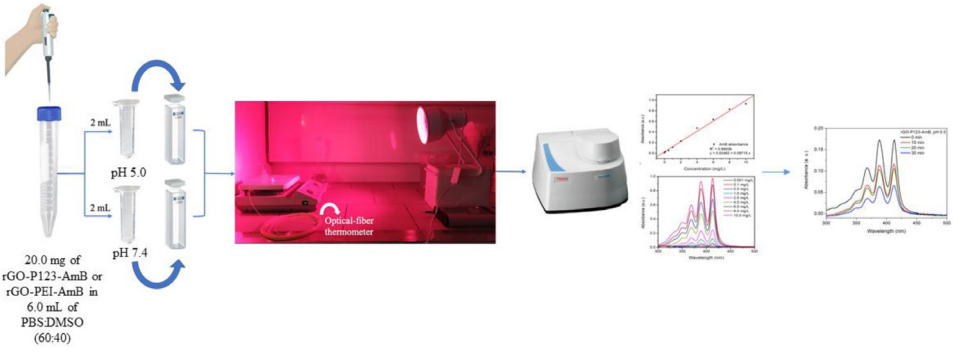

Fig. 18. Schematic representation of the procedure employed for the AmB release studies from rGO-P123-AmB and rGO-PEI-AmB trigged by NIR light at pH 5.0 and 7.4. The same experiments on both pH values were carried out without NIR light irradiation (control experiment).

2.4. Amphotericin B (AmB) release studies triggered by NIR light stimulus using an infrared lamp

AmB release studies from rGO-P123-AmB and rGO-PEI-AmB were carried out by irradiating their dispersions in PBS:DMSO (60:40) with near-infrared (NIR) light from an infrared lamp (with 90% of energy transmitted as infrared with a pronounced peak at 1000 nm, 150 W). The same studies were conducted in the absence of NIR light stimulus (control experiment). For these experiments, 20 mg of rGO-P123-AmB or rGO-PEI-AmB was dispersed in 6 mL of a mixture of PBS:DMSO (60:40) and then, 2 mL of each dispersion was transferred to a safe-lock microcentrifuge tube and the pH values adjusted to 5.0 and 7.4, respectively, using 0.5 mol L^{-1} HCl. The dispersions were centrifuged (Thermo Scientific, Heraeus Fresco 21 Microcentrifuge) at 14800 rpm for 5 min, the supernatants transferred to quartz cuvettes and the absorbance measured in a UV-Vis spectrophotometer (initial point). Then, 2 mL of fresh PBS:DMSO (60:40) solutions at pH 5.0 and 7.4, respectively, were added to the remaining solids present in the microcentrifuge tubes. The dispersions were transferred again to quartz cuvettes, and in one of them NIR light was irradiated with the lamp at a distance of 64 cm for 10 min under stirring (first cycle) and the absorbances were measured in the UV-Vis spectrophotometer (Thermo Scientific Evolution 60S). This distance was employed in order to avoid excessive heating of the dispersions during the experiments. The temperature of the dispersions irradiated with NIR light was monitored using an optical-fiber thermometer (NomadTM – Neoptix) inserted in the cuvettes. Next, these dispersions were irradiated for further 10 min for two times, which corresponds to the points of 20 min (second cycle) and 30 min (third cycle) of the release profiles. The other sample remained stirring for the same period of time without light irradiation (control experiment) and the absorbance was also measured to obtain the passive diffusion of AmB from rGO-P123-AmB and rGO-PEI-AmB. These procedures were repeated three times for both pH values (see schematic representation of the procedure in Fig. 18). The amounts of AmB released from the materials were determined using the standard curve prepared by measuring a series of concentrations of AmB solutions in PBS:DMSO (60:40) at $\lambda = 389$ nm (Fig. 17).

3. Biological Assays

3.1. Parasite and macrophage cell line

Leishmania amazonensis WHOM/BR/75/JOSEFA strain was used in this study. It was isolated in 1975 from a patient with diffuse cutaneous leishmaniasis by Dr. Cesar A. Cuba-Cuba (University of Brasília, Brazil) and kindly provided by the *Leishmania* Collection of the Oswaldo Cruz

Institute (Code IOCL 0071 - FIOCRUZ). RAW 264.7 macrophages is a cell line from the *Mus musculus* mouse immortalized from a tumor induced by the Abelson murine leukemia virus.

3.2. Preparation of materials for biological assays

The materials and the AmB drug were dissolved in a solution of PBS:DMSO (60:40). The maximum concentration of the DMSO in the cultures did not exceed 0.5 %, which is a concentration that does not affect cell growth.

3.3. Cytotoxicity assay

CellTiter 96 Aqueous MTS/PMS Assay (Promega, WI, USA) was used to analyse the cytotoxicity of the control macrophages and macrophages treated with AmB-unloaded and AmB-loaded systems. This assay is a semi-automatic colorimetric test where the tetrazolium salt is bioreduced by the dehydrogenases of viable cells to a product called formazan [20]. RAW 264.7 Macrophages were cultured at a cell density of 1×10^5 cells mL^{-1} in a 96-well plate. After 24 h, two concentrations (5 and 15 μg mL^{-1}) of rGO-P123, rGO-P123-AmB, rGO-PEI and rGO-PEI-AmB were added to the cultures and the medium changed every 24 h. Cytotoxicity was assessed every 24 h of treatment up to maximum treatment time of 72 h; for this experiment, 20 µL of a mixture of 333 µg mL^{-1} MTS and 25 µM PMS were added for each 100 µL of culture medium. After 4 h of incubation, absorbance readings were performed using a wavelength of 490 nm in a microplate reader (Spectra Max Paradigme from Molecular Devices). Each group was analyzed in triplicate. The interactions of the RAW264.7 macrophages with rGO-PEI, rGO-P123, rGO-PEI-AmB and rGO-P123-AmB are represented in Fig. 15.

3.4. Evaluation of antiproliferative effects in Leishmania amazonensis promastigotes in the presence and absence of NIR light

To evaluate the antiproliferative effects in *Leishmania amazonensis* promastigotes, growth curves were initiated with an inoculum of 1.0×10^6 cells mL^{-1} in M199 culture medium supplemented with 10% fetal bovine serum. After 24 h of growth, different experimental groups were designed: (i) 0.46 µg mL^{-1} AmB; (ii) 5.35 µg mL^{-1} of rGO-PEI and (iii) 5.35 µg mL^{-1} of rGO-PEI-AmB. The concentrations of the materials were calculated taking into account the amount of AmB loaded in order to have AmB concentration of approximately 0.46 µg mL^{-1} per culture, which is the IC_{50} value for AmB. The experimental groups were carried out in duplicate; half of the cultures was irradiated with NIR light, and the other half was not. For this, after 6 h of the addition of the materials, the irradiated groups of culture were positioned at a distance of 64 cm from the infrared lamp. The distance between cultures and the lamp was calculated in order to maintain the cell culture temperature at 25 °C. Then, the cultures were irradiated for three consecutive periods of 10 min (Fig. 19) every 24 h until the end of the treatment. The cells were cultured for a total of 96 h, with cell density calculated every 24 h, by counting the number of cells in a Neubauer chamber using contrast-phase light microscopy.

3.5. Scanning Transmission Electron Microscopy in Scanning Electron Microscopy (STEM-IN-SEM) of Leishmania amazonensis promastigotes treated with rGO-PEI and rGO-PEI-AmB

Promastigotes control and treated with AmB, rGO-PEI and rGO-PEI-AmB were washed in PBS (pH 7.2) and fixed in 2.5% glutaraldehyde in 0.1 M sodium cacodylate buffer, pH 7.2, for 1 h.

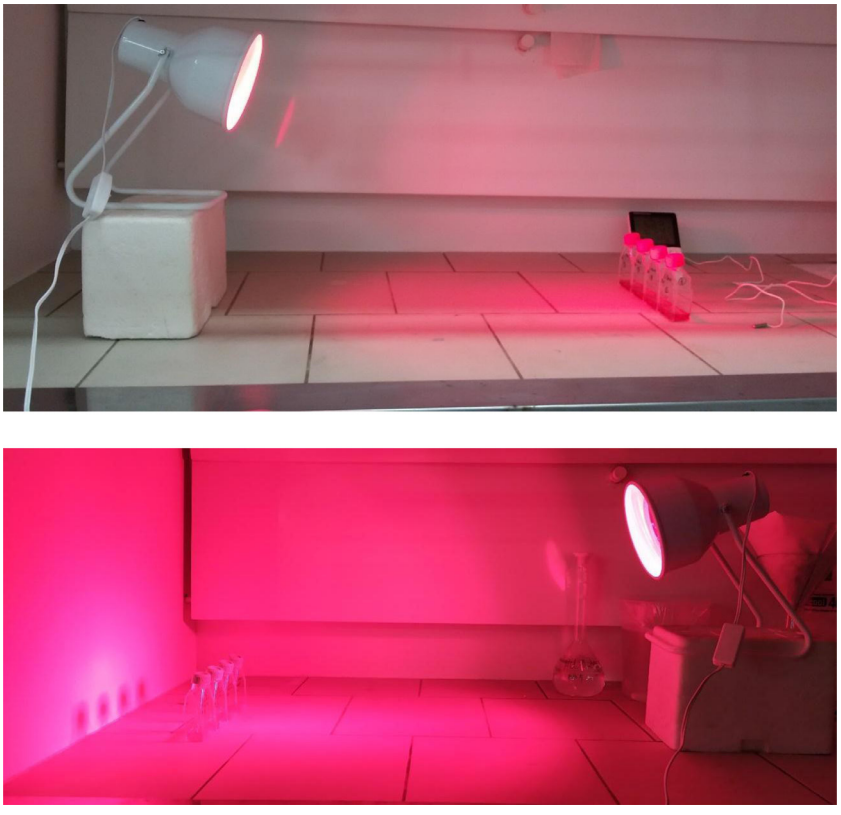

Fig. 19. Cell cultures irradiated with NIR light from an IR lamp for three periods of 10 min.

Then, cells were post-fixed in a solution containing 1 % osmium tetroxide (OsO_4), 1.25 % potassium ferricyanide, 5 mM calcium chloride ($CaCl_2$) in 0.1 M sodium cacodylate buffer at room temperature and protected from light for 30 min. Then, the samples were dehydrated in graded acetone solutions (25, 50, 75, 95 and 100% for 10 min each) and embedded in Epon resin. The ultrathin section (approximately 60 nm) was performed in an ultramicrotome (RMC PT-PC); ultrathin sections were stained with uranyl acetate (5%) for 45 min and lead citrate (Reynolds solution) for 5 min and analysed through SEM (TESCAN VEGA 3 LMU) operating in STEM mode with an acceleration voltage of 25 kV.

CRediT Author Statement

Letícia S. Vitorino: experimental work up, spectroscopic, thermal characterization, drug release studies of the materials, biological studies, data curation and first draft writing. **Thiago C. dos Santos**: experimental work up, spectroscopic, thermal characterization, data curation and first draft writing. **Isabela A. A. Bessa**: spectroscopic, thermal characterization and drug release studies of the materials and data curation. **Evelyn C. S. Santos**: experimental work up, spectroscopic characterization and drug release studies of the materials, data curation and first draft writing. **Brunno R. F. Verçoza:** biological studies, data curation and first draft writing. **Luiz Augusto S. de Oliveira**: biological studies and data curation. **Juliany C. F. Rodrigues:** biological

studies, data curation and first draft writing. **Célia M. Ronconi:** conceptualization, formal analysis, project administration, supervision and final writing and review.

Declaration of Competing Interest

The authors declare that they have no known competing financial interests or personal relationships that could have appeared to influence the work reported in this paper.

Acknowledgments

This work was financially supported by the Brazilian agencies National Council for Scientific and Technological Development (CNPq, Universal grant numbers 434141/2018-6, 423086/2018-9 and 420016/2018-0, C.M.R. research fellowship grant number 313799/2017-2), Brazilian Federal Agency for Support and Evaluation of Graduate Education (CAPES, L. S. V., T. C. S. and E. C. S. S. fellowship) and Rio de Janeiro Research Foundation (FAPERJ, Sediadas grant number E-26/010.101133/2018, Cientistas do Nosso Estado grant number E-26/202.629/2019, Redes de Pesquisa em Nanotecnologia no Estado do Rio de Janeiro grant number E-26/010.000981/2019, Bolsa Nota 10 L. S. V. grant number E-26/200.871/2019 and I. A. A. B. fellowship E-26/200.277/2018). We are grateful to the Molecular Spectroscopy (http://www.uff.br/lame/), Material Characterization (http://www.uff.br/lamate/) and X-Ray Diffraction (http://ldrx.sites.uff.br) Multiuser Laboratories from Universidade Federal Fluminense (UFF). The authors also thank MSc Alan Moraes for assistance with the TEM images and Cauê Nogueira with the SEM images.

References

[1] L.S. Vitorino, T.C. dos Santos, I.A.A. Bessa, E.C.S. Santos, B.R.F. Verçoza, L.A.S. de Oliveira, J.C.F. Rodrigues, C.M. Ronconi, Amphotericin-B-Loaded Polymer-Functionalized Reduced Graphene Oxides for Leishmania amazonensis Chemo-Photothermal Therapy, Colloid Surface B 209 (2022) 112169–112178 In Press, doi:10.1016/j.colsurfb.2021.112169.

[2] T.C. dos Santos, E.C.S. Santos, J.P. Dias, J. Barreto, F.L. Stavale, C.M. Ronconi, Reduced graphene oxide as an excellent platform to produce a stable Brønsted acid catalyst for biodiesel production, Fuel 256 (2019) 115793–115802, doi:10.1016/j.fuel.2019.115793.

[3] J.T. Robinson, S.M. Tabakman, Y. Liang, H. Wang, H.S. Casalongue, D. Vinh, H. Dai, Ultrasmall reduced graphene oxide with high near-infrared absorbance for photothermal therapy, J. Am. Chem. Soc. 133 (2011) 6825–6831, doi:10.1021/ja2010175.

[4] A. Raval, S.A. Pillai, A. Bahadur, P. Bahadur, Systematic characterization of Pluronic® micelles and their application for solubilization and in vitro release of some hydrophobic anticancer drugs, J. Mol. Liq. 230 (2017) 473–481, doi:10.1016/j.molliq.2017.01.065.

[5] A.V. Kabanov, P. Lemieux, S. Vinogradov, V. Alakhov, Pluronic® block copolymers: Novel functional molecules for gene therapy, Adv. Drug Deliv. Rev. 54 (2002) 223–233, doi:10.1016/S0169-409X(02)00018-2.

[6] H. Hu, J. Yu, Y. Li, J. Zhao, H. Dong, Engineering of a novel pluronic F127/graphene nanohybrid for pH responsive drug delivery, J. Biomed. Mater. Res. - Part A. 100 A (2012) 141–148, doi:10.1002/jbm.a.33252.

[7] H. Liu, T. Kuila, N.H. Kim, B.-C. Ku, J.H. Lee, In situ synthesis of the reduced graphene oxide-polyethyleneimine composite and its gas barrier properties, J. Mater. Chem. A. 1 (2013) 3739–3746, doi:10.1039/c3ta01228j.

[8] D. Pakulski, W. Czepa, S. Witomska, A. Aliprandi, P. Pawluć, V. Patroniak, A. Ciesielski, P. Samorì, Graphene oxide-branched polyethylenimine foams for efficient removal of toxic cations from water, J. Mater. Chem. A. 6 (2018) 9384–9390, doi:10.1039/c8ta01622d.

[9] Q. Liu, Y. Zhou, M. Li, L. Zhao, J. Ren, D. Li, Z. Tan, K. Wang, H. Li, M. Hussain, L. Zhang, G. Shen, J. Zhu, J. Tao, Polyethylenimine hybrid thin-shell hollow mesoporous silica nanoparticles as vaccine self-adjuvants for cancer immunotherapy, ACS Appl. Mater. Interfaces. 11 (2019) 47798–47809, doi:10.1021/acsami.9b19446.

[10] P. Pankongadisak, E. Tsekoura, O. Suwantong, H. Uludağ, Electrospun gelatin matrices with bioactive pDNA polyplexes, Int. J. Biol. Macromol. 149 (2020) 296–308, doi:10.1016/j.ijbiomac.2020.01.252.

[11] R.K. Layek, M.E. Uddin, N.H. Kim, A.K. Tak Lau, J.H. Lee, Noncovalent functionalization of reduced graphene oxide with pluronic F127 and its nanocomposites with gum arabic, Compos. Part B Eng. 128 (2017) 155–163, doi:10.1016/j.compositesb.2017.07.010.

[12] X. Zhang, Y. Liu, C. Sun, H. Ji, W. Zhao, S. Sun, C. Zhao, Graphene oxide-based polymeric membranes for broad water pollutant removal, RSC Adv 5 (2015) 100651–100662, doi:10.1039/c5ra20243d.

[13] C. Liu, H. Liu, C. Lu, K. Tang, Y. Zhang, Polyethyleneimine-modified graphene oxide/PNIPAm thermoresponsive hydrogels with rapid swelling/deswelling and improved mechanical properties, J. Mater. Sci. 52 (2017) 11715–11724, doi:10.1007/s10853-017-1301-5.

[14] M.T.H. Aunkor, I.M. Mahbubul, R. Saidur, H.S.C. Metselaar, The green reduction of graphene oxide, RSC Adv 6 (2016) 27807–27825, doi:10.1039/c6ra03189g.
[15] T.C. dos Santos, C.M. Ronconi, Self-assembled 3D mesoporous graphene oxides (MEGOs) as adsorbents and recyclable solids for CO_2 and CH_4 capture, J. CO_2 Util. 20 (2017) 292–300, doi:10.1016/j.jcou.2017.05.018.
[16] M. Hashemi, M. Omidi, B. Muralidharan, H. Smyth, M.A. Mohagheghi, J. Mohammadi, T.E. Milner, Evaluation of the Photothermal Properties of a Reduced Graphene Oxide/Arginine Nanostructure for Near-Infrared Absorption, ACS Appl. Mater. Interfaces. 9 (2017) 32607–32620, doi:10.1021/acsami.7b11291.
[17] Y. Liu, L. Xu, J. Liu, X. Liu, C. Chen, G. Li, Y. Meng, Graphene oxides cross-linked with hyperbranched polyethylenimines: Preparation, characterization and their potential as recyclable and highly efficient adsorption materials for lead(II) ions, Chem. Eng. J. 285 (2016) 698–708, doi:10.1016/j.cej.2015.10.047.
[18] N.I. Kovtyukhova, P.J. Ollivier, B.R. Martin, T.E. Mallouk, S.A. Chizhik, E.V Buzaneva, A.D. Gorchinskiy, Layer-by-Layer Assembly of Ultrathin Composite Films from Micron-Sized Graphite Oxide Sheets and Polycations, Chem. Mater. 11 (1999) 771–778.
[19] Y. Li, J. Liu, H. Dong, G. Liu, H. Hu, Engineering of a Pluronic F127 functionalized magnetite/graphene nanohybrid for chemophototherapy, Nanotechnology 25 (2014) 1–10, doi:10.1088/0957-4484/25/6/065602.
[20] C. Henriques, T.L.B. Moreira, C. Maia-Brigagão, A. Henriques-Pons, T.M.U. Carvalho, W. de Souza, Tetrazolium salt based methods for high-throughput evaluation of anti-parasite chemotherapy, Anal. Methods. 3 (2011) 2148–2155, doi:10.1039/c1ay05219e.